Plasma identification in fusion devices, Models and Methods for plasma control in fusion devices

SECTION IV

PLASMA IDENTIFICATION IN FUSION DEVICES

M. Bagatin, P.Bettini, G. Chitarin, M. De Magistris, D. Desideri, A. Formisano, R. Fresa, R. Martino, R. Martone, A. Pironti, A. Stella, F. Trevisan, L. Zabeo

Abstract

The identification of plasma parameters from suitable sets of measurements is a key topic in the thermonuclear fusion research. Most of the information relevant to the plasma shape and position control is usually gained via external magnetic measurements, although information related to internal distribution of current density is not accessible in this way. A number of possible approaches to fast identification of plasma geometrical parameters have been proposed; the equivalent currents method will be analysed here with some detail, together with an alternative model based on a very simple plasma current model.

To estimate other, non geometrical parameters, but also to improve the geometrical identification, alternative measurements can be profitably used, coupled with the magnetic measurements. As an example, polarimetric measurements will be analysed here, together with an alternative method for the identification of magnetic field configurations based on the trajectories of charged particles.

1. INTRODUCTION

In the toroidal experimental devices for plasma magnetic confinement a set of toroidal field coils is devoted to the plasma confinement and stabilisation and a set of poloidal field coils is devoted to the plasma break-down and position/shape control. The latter are driven by an active system, that controls the plasma shape by modifying the poloidal field map on the basis of an estimate of the actual plasma configuration [1, 2]. Plasma shape identification appears then a critical issue, because its promptness and accuracy hardly impact the effectiveness of control action.

Due to the lack of direct plasma geometry information, the plasma shape/position identification is usually performed by considering external measurements, providing indirect information on the plasma geometry, and then solving

a suitably formulated inverse problem. In such formulations, the electromagnetic behaviour of the plasma is typically represented in terms of some simplified representation; the model can possibly include MHD equilibrium equations.

The most common approaches are based on the representation of the electromagnetic plasma behaviour in terms of equivalent sources (e.g. filamentary currents or magnetic multipoles); others adopt some kind of data interpolation (neural networks, function parameterization).

In the following a brief description of a couple of possible models is presented, based alternatively on a simplified MHD model and on an equivalent currents representation of the plasma current. For both of the models the results obtained in the course of the project are reported, together with a brief discussion about their perspectives.

2. DIAGNOSTIC SYSTEMS

The fusion devices diagnostics are usually very complex systems, including many different probing systems, based on a number of different measurements schemes. Anyway, the main sources of information to recover the plasma electromagnetic behaviour are based on magnetic measurements, including either flux and field probes, positioned outside the plasma chamber. Some additional information can also be gained with non-magnetic measurement systems, such as those based on motional Stark effect or the polarimetric probes, based on the Faraday rotation effect [3, 4, 5].

Magnetic probes are well known devices, and will not be discussed any more here. On the other hand, in recent years polarimeter systems, based on the rotation of the polarisation plane (Faraday rotation) undergone by a probing laser beam crossing the magnetised plasma, are becoming routinely employed on most significant experiments. The Faraday rotation angle $\Delta\Psi$ undergone by the beam propagating along the z direction is given by:

$$\Delta\Psi(x) = A\lambda^2 \int_{z_1}^{z_2} n_e(x,z) B_{\theta\parallel}(x,z) dz \tag{2.1}$$

where A is a dimensional constant depending on the device, λ is the laser wavelength, n_e is the plasma electron density, $B_{\theta//}$ is the poloidal field component along the z direction, x is the horizontal coordinate.

The electron density radial profile is provided by other diagnostics. Note that usually a number of polarimeters are allocated parallel to each other, and the measurements are simultaneously performed, providing in this way useful information about the magnetic field map in the whole plasma region.

In principle, starting from the polarimetric measurements, the complete plasma current profile can be reconstructed by means of an inversion algorithm, eventually coupled with a proper plasma model, but, due to an unfavourable signal to noise ratio (in the order of few tens), a reliable inversion based on polarimeters only would require both a large number of chords and a heavy computational effort. However these measurements provide significant perspectives in real time plasma identification if coupled with magnetic measurement based reconstruction procedures.

3. IDENTIFICATION METHODS BASED ON A MHD PLASMA MODEL

Advanced scenarios of the plasma performance relies on the possibility of achieving a real time control of the current profiles in the bulk plasma, in order to optimise the confinement properties. Reliable and efficient determination of plasma current profiles is thus a crucial issue. High-beta and low-field configurations, like Reversed Field Pinches (RFPs), in which the magnetic field configuration inside the plasma is mainly driven by plasma current itself, can therefore constitute a suitable benchmark to test the reliability and robustness of current profile reconstruction algorithms.

An algorithm inferring the current profile has been developed in the frame of the research project [6]. The tool is particularly efficient thanks to the synergy resulting from the integration of external magnetic and internal non-magnetic measurements. The technique has been implemented and experimentally validated on the RFP machine RFX. The activity has been carried out along two steps. At first an off-line algorithm has been developed, independently of the computational time, and then it has been modified in a fast tool, aimed at real-time applications.

3.1. OFF-LINE IDENTIFICATION TECHNIQUE

The approach is based on a relatively simple MHD plasma equilibrium model [7], being magnetic external and FIR internal measurements superimposed as additional constraints. A simplified solution of the MHD equilibrium equations in toroidal axisymmetric geometry can be found in the case of zero pressure gradient and ideal magnetic flux conservation at the conducting shell. In this case the resulting force-free magnetic profile satisfies the equations:

$$J_\varphi = B_\varphi\, \alpha/\mu_0 \quad ; \quad J_\theta = B_\theta\, \alpha/\mu_0 \tag{3.1.1}$$

where $\alpha=\mu_0(\boldsymbol{J}\cdot\boldsymbol{B})/B^2$ is a scalar quantity considered constant along the poloidal field lines. The solution of equations (3.1.1) is derived considering a discretised machine

In principle, starting from the polarimetric measurements, the complete plasma current profile can be reconstructed by means of an inversion algorithm, eventually coupled with a proper plasma model, but, due to an unfavourable signal to noise ratio (in the order of few tens), a reliable inversion based on polarimeters only would require both a large number of chords and a heavy computational effort. However these measurements provide significant perspectives in real time plasma identification if coupled with magnetic measurement based reconstruction procedures.

3. IDENTIFICATION METHODS BASED ON A MHD PLASMA MODEL

Advanced scenarios of the plasma performance relies on the possibility of achieving a real time control of the current profiles in the bulk plasma, in order to optimise the confinement properties. Reliable and efficient determination of plasma current profiles is thus a crucial issue. High-beta and low-field configurations, like Reversed Field Pinches (RFPs), in which the magnetic field configuration inside the plasma is mainly driven by plasma current itself, can therefore constitute a suitable benchmark to test the reliability and robustness of current profile reconstruction algorithms.

An algorithm inferring the current profile has been developed in the frame of the research project [6]. The tool is particularly efficient thanks to the synergy resulting from the integration of external magnetic and internal non-magnetic measurements. The technique has been implemented and experimentally validated on the RFP machine RFX. The activity has been carried out along two steps. At first an off-line algorithm has been developed, independently of the computational time, and then it has been modified in a fast tool, aimed at real-time applications.

3.1. OFF-LINE IDENTIFICATION TECHNIQUE

The approach is based on a relatively simple MHD plasma equilibrium model [7], being magnetic external and FIR internal measurements superimposed as additional constraints. A simplified solution of the MHD equilibrium equations in toroidal axisymmetric geometry can be found in the case of zero pressure gradient and ideal magnetic flux conservation at the conducting shell. In this case the resulting force-free magnetic profile satisfies the equations:

$$J_\varphi = B_\varphi \, \alpha/\mu_0 \quad ; \quad J_\theta = B_\theta \, \alpha/\mu_0 \tag{3.1.1}$$

where $\alpha=\mu_0(\boldsymbol{J}\cdot\boldsymbol{B})/B^2$ is a scalar quantity considered constant along the poloidal field lines. The solution of equations (3.1.1) is derived considering a discretised machine

geometry (Fig. 3.1.1) representing all the passive and active conductors surrounding the plasma (vessel, shell, toroidal and poloidal windings).

The discretised plasma and shell currents are unknown, while the vessel current and the windings currents are derived from measurements and the α profile is expressed as a function of the normalized poloidal flux $\tilde{\Psi}$ (equal to one where the poloidal flux is minimum, and equal to zero where is maximum). As a first attempt, a parabolic expression for $\alpha(\tilde{\Psi})$ has been used:

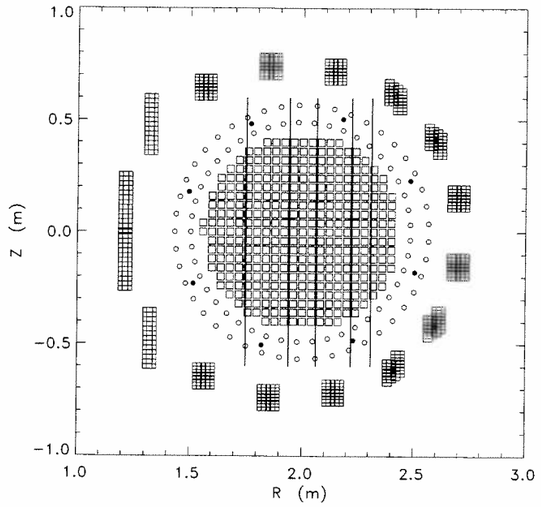

Fig. 3.1.1. Discretisation of toroidal plasma current into squared cross-section conductors and discretisation of vessel, shell and field shaping coils into filamentary currents. The vertical polarimeter paths (five chords) and the magnetic probe locations (eight solid points) are also indicated.

(3.1.2) $$\alpha=\alpha(\tilde{\Psi})=\alpha_O(1-\tilde{\Psi}^{\beta}).$$

The poloidal currents inside the plasma are represented by axisymmetric current sheets, having the same shape of the poloidal flux surfaces. The poloidal current sheets in the plasma are unknowns identified by means of the poloidal flux functions, which in turn are univocally determined by the distribution of the toroidal filamentary currents. Additional current sheets account for the vessel and external winding poloidal currents.

The set of equations on the discretised currents corresponding to equations (3.1.1) are coupled to the additional constraints set derived from the measured total plasma current, the condition of null total shell current and the ideal flux conserving condition associated to the shell.

In equation (3.1.2) the parameter α_O is determined by the external measurements, whereas an initial guess value is assumed for β and then iteratively adjusted to match the toroidal field winding current. The model provides as output parameters the discretised toroidal and poloidal plasma currents and the shell toroidal filamentary currents, and therefore a first estimate of the field profiles inside the plasma.

The magnetic field and the polarimetric measurements are integrated into the equilibrium model by writing one supplementary equation for each of the magnetic probes and for each of the polarimeter chords. Each of these equations expresses the relationship between the unknown current in the plasma filaments J_φ and one of the measured quantities. In the case of the pick-up coils, the measured quantities are B_{probe}, and the equations have the following form:

(3.1.3) $$[B_{probe}] = [A]\,[J_\varphi]$$

where matrix $[A]$ depends on the discretised machine geometry by way of the Green functions.

The measured Faraday rotation angles $\Delta\Gamma_{chord}$ are related to the poloidal field component along the chords by the following matricial relationship:

(3.1.4) $$[\Delta\Gamma_{chord}] = [C]\,[D]\,[J_\varphi]$$

where $[C]$ is a geometrical matrix determined by the topology of the chords and $[D]$ includes the experimental density profile.

During the tests, up to 16 equations have been used for the poloidal field pick–up coils and 5 for the polarimeter chords. These equations, written together with those expressing the MHD equilibrium model, constitute an over-determined system. The system is solved using the Singular Value Decomposition algorithm and applying a regularization technique based on the truncation of the smallest singular values. The exponent β in equation (3.1.2) is arbitrarily assumed and then iteratively changed, until a prescribed matching of the equations is obtained.

In order to assess the capability of the model and of both magnetic and polarimetric measurements to give valuable information on internal magnetic field distribution, a number of different runs of the code have been performed. Different relative weights have been attributed to the matrices coefficients, in consideration of the different accuracy of the relevant measurement techniques. The relative weights have been chosen in such a way to stop the iteration procedure after the achievement of a relative accuracy of 1.5% for magnetic pick-up coils and of 15 % for the Faraday rotation angle.

The magnetic field profiles computed with the equilibrium model, using as input parameters only the plasma current and the toroidal loop voltages in a RFX discharge is illustrated in Fig. 3.1.2 (curves *(a)* with reference to RFX shot #14170).

In equation (3.1.2) the parameter α_O is determined by the external measurements, whereas an initial guess value is assumed for β and then iteratively adjusted to match the toroidal field winding current. The model provides as output parameters the discretised toroidal and poloidal plasma currents and the shell toroidal filamentary currents, and therefore a first estimate of the field profiles inside the plasma.

The magnetic field and the polarimetric measurements are integrated into the equilibrium model by writing one supplementary equation for each of the magnetic probes and for each of the polarimeter chords. Each of these equations expresses the relationship between the unknown current in the plasma filaments J_φ and one of the measured quantities. In the case of the pick-up coils, the measured quantities are B_{probe}, and the equations have the following form:

$$[B_{probe}] = [A]\,[J_\varphi] \tag{3.1.3}$$

where matrix $[A]$ depends on the discretised machine geometry by way of the Green functions.

The measured Faraday rotation angles $\Delta\Gamma_{chord}$ are related to the poloidal field component along the chords by the following matricial relationship:

$$[\Delta\Gamma_{chord}] = [C]\,[D]\,[J_\varphi] \tag{3.1.4}$$

where $[C]$ is a geometrical matrix determined by the topology of the chords and $[D]$ includes the experimental density profile.

During the tests, up to 16 equations have been used for the poloidal field pick–up coils and 5 for the polarimeter chords. These equations, written together with those expressing the MHD equilibrium model, constitute an over-determined system. The system is solved using the Singular Value Decomposition algorithm and applying a regularization technique based on the truncation of the smallest singular values. The exponent β in equation (3.1.2) is arbitrarily assumed and then iteratively changed, until a prescribed matching of the equations is obtained.

In order to assess the capability of the model and of both magnetic and polarimetric measurements to give valuable information on internal magnetic field distribution, a number of different runs of the code have been performed. Different relative weights have been attributed to the matrices coefficients, in consideration of the different accuracy of the relevant measurement techniques. The relative weights have been chosen in such a way to stop the iteration procedure after the achievement of a relative accuracy of 1.5% for magnetic pick-up coils and of 15 % for the Faraday rotation angle.

The magnetic field profiles computed with the equilibrium model, using as input parameters only the plasma current and the toroidal loop voltages in a RFX discharge is illustrated in Fig. 3.1.2 (curves *(a)* with reference to RFX shot #14170).

The introduction of the pick-up coils additional constraints does not normally cause a remarkable change in the computed profiles (curves *(b)*), which are not too far from the previous one.

A different situation arises when the integral measurements given by the polarimetric diagnostic are integrated into the code. The internal measurements indeed oblige the code to converge to a solution (curves *(c)* in Fig. 3.1.2), which can be remarkably different from the one obtained without the polarimetric constraints.

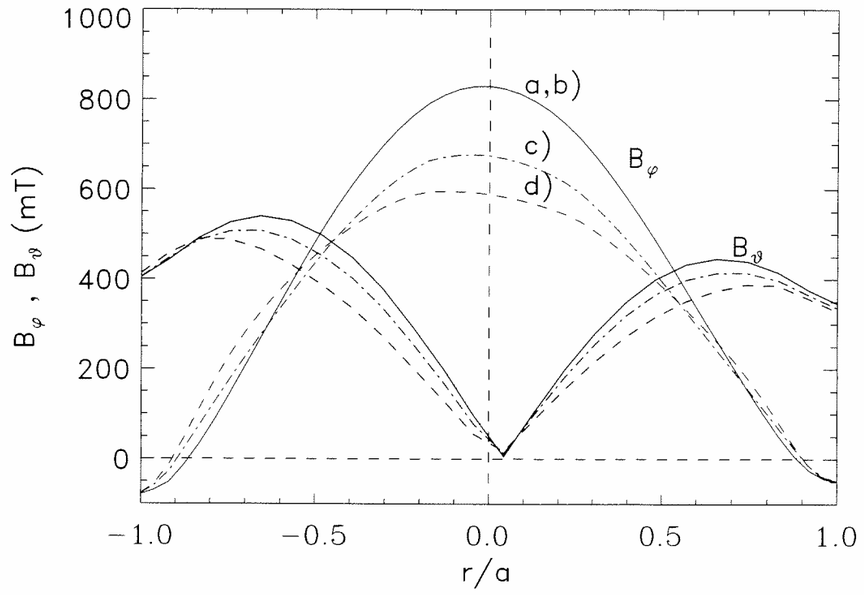

Fig. 3.1.2. Poloidal and toroidal magnetic field profiles computed by the model in three different situations: a) only equilibrium conditions; b) with pickup coils' additional constraints; c) with polarimetric measurements constraints and standard parabolic $\alpha(\tilde{\Psi})$ profile; d) with polarimetric measurements constraints and hollow $\alpha(\tilde{\Psi})$ profile.

It has been found that for several shots, once the polarimetric constraints were inserted, the convergence of the code degraded remarkably. Since for almost all the cases investigated the most difficult region to match is the one crossed by the outermost chords, a more general hollow profile of α has been implemented, in order to improve the degrees of freedom in the region close to the boundary. The following four-parameter shaping function has been used:

(3.1.5) $$\alpha=\alpha(\tilde{\Psi})=\alpha_0(1-\tilde{\Psi}^{\gamma})+\alpha_1(\tilde{\Psi}^{\gamma}-\tilde{\Psi}^{\beta}),$$

with α_1 greater than α_0, β greater than γ. With this more relaxed constraint the computed field structure undergoes a further appreciable modification, which is evidenced by curves *(d)* in Figure 3.2.

3.2. FAST IDENTIFICATION TOOL

A simplified version of the code has been also implemented, with the aim to drastically reduce the code execution time, without leading to an excessive loss of reliability and precision [8].

The main simplification that has been introduced consists in the assumption of a constant density radial profile given by the interferometer central chords, data necessary for the polarimeter. Moreover the geometry of the discretised currents has been completely fixed, allowing an extensive use of pre-calculated matrices. Finally, the parameters in the parabolic relation (equation (3.1.2)) are iteratively changed within preselected limits, starting from an initial value for α_0 computed from the external measurements and an initial guess for β.

An automatic procedure was written in order to easily vary the number of the discretised code outputs ($N_{p\varphi}$, $N_{p\theta}$ and $N_{s\varphi}$ are respectively the number of the plasma toroidal, poloidal and shell toroidal filamentary currents). This is aimed at assessing the optimised number of unknowns, as a compromise between the best resolution in the results and minimum code reconstruction time. In the present version of the code, $N_{p\varphi}$, $N_{p\theta}$ and $N_{s\varphi}$ have been set at 376, 100 and 45 respectively.

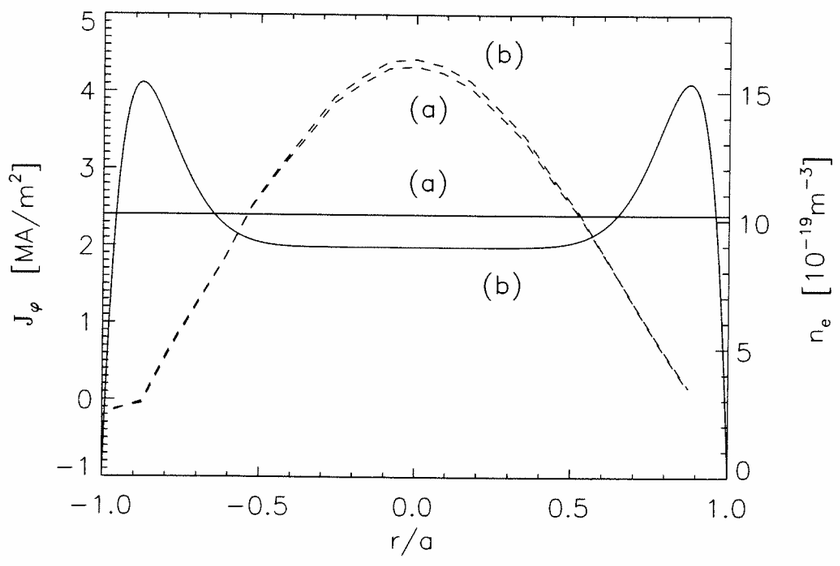

FIG. 3.2.1. RFX shot # 14164 at 29 ms after the plasma current start time. Reconstructed toroidal density current J_φ (dashed line a) with constant electron density radial profile n_e (solid line a); reconstructed J_φ (dashed line b) with identified interferometer n_e radial profile (solid line b).

with α_I greater than α_0, β greater than γ. With this more relaxed constraint the computed field structure undergoes a further appreciable modification, which is evidenced by curves *(d)* in Figure 3.2.

3.2. FAST IDENTIFICATION TOOL

A simplified version of the code has been also implemented, with the aim to drastically reduce the code execution time, without leading to an excessive loss of reliability and precision [8].

The main simplification that has been introduced consists in the assumption of a constant density radial profile given by the interferometer central chords, data necessary for the polarimeter. Moreover the geometry of the discretised currents has been completely fixed, allowing an extensive use of pre-calculated matrices. Finally, the parameters in the parabolic relation (equation (3.1.2)) are iteratively changed within preselected limits, starting from an initial value for α_0 computed from the external measurements and an initial guess for β.

An automatic procedure was written in order to easily vary the number of the discretised code outputs ($N_{p\varphi}$, $N_{p\theta}$ and $N_{s\varphi}$ are respectively the number of the plasma toroidal, poloidal and shell toroidal filamentary currents). This is aimed at assessing the optimised number of unknowns, as a compromise between the best resolution in the results and minimum code reconstruction time. In the present version of the code, $N_{p\varphi}$, $N_{p\theta}$ and $N_{s\varphi}$ have been set at 376, 100 and 45 respectively.

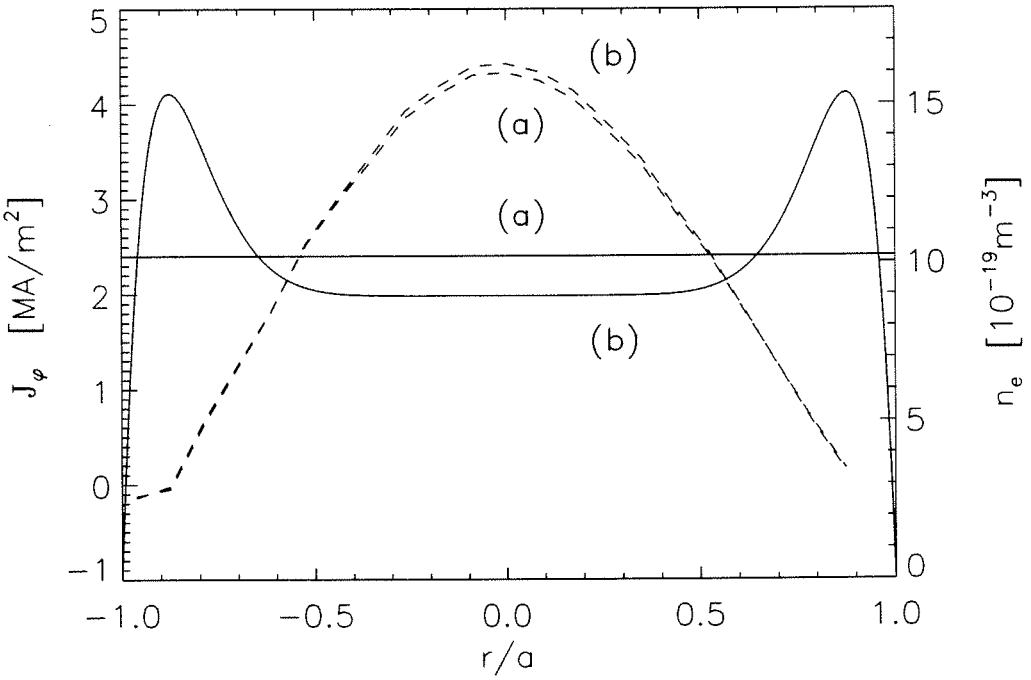

FIG. 3.2.1. RFX shot # 14164 at 29 ms after the plasma current start time. Reconstructed toroidal density current J_φ (dashed line a) with constant electron density radial profile n_e (solid line a); reconstructed J_φ (dashed line b) with identified interferometer n_e radial profile (solid line b).

In Fig. 3.2.1 an example of internal profile reconstruction is reported. Dashed line *(a)* represents the reconstructed toroidal density current J_φ obtained by assuming a constant electron density n_e radial profile (solid line *(a)*), while dashed line *(b)* represents the reconstructed J_φ obtained by using the identified electron density radial profile given by the interferometer (solid line *(b)*). The comparison shows that the simplifying assumption of flat density profile seems quite acceptable.

The time required for profile reconstruction is presently about one second on a 600 MHz Alpha® processor.

4. IDENTIFICATION METHODS BASED ON EQUIVALENT PLASMA REPRESENTATIONS

Due to the tight promptness requirements, the plasma magnetic boundary identification for control purposes is typically performed by using external magnetic measurements, provided by a set of magnetic probes, either pick-up coils and toroidal coaxial loops, located around the plasma. From the acquired data and without the use of plasma models, by adopting a suitable approximated representation of the plasma effect, the magnetic boundary can be identified. To this purpose two classical representations can be used: the Multipole Harmonic Expansion and the Equivalent Currents Method.

4.1. MULTIPOLE HARMONIC EXPANSION

The method is based on the harmonic expansion of the flux distribution produced by the plasma current in terms of a truncated series of toroidal eigenfunctions. Unlike the other harmonic expansion techniques, the pivotal point for the harmonic expansion is chosen as the plasma current centroid, determined as a suitable moment of a set of filamentary currents which approximates the plasma current magnetic effects. In this way, the algorithm makes a trade-off between the accurateness in the plasma shape reconstruction and the computational burden, so that it can be conveniently used in feedback schemes for plasma shape control.
Starting from the measured currents in the external coils and from a set of flux and field measurements, the last closed flux surface inside the vessel can be estimated.

4.2. EQUIVALENT CURRENTS METHOD

One of the most effective approaches to such a problem is based on the approximate representation of the plasma current density through an expansion in terms of "equivalent currents" (EC), in such a way that at least the first moments of the magnetic field are correctly represented [9, 10, 11]. More precisely, the actual plasma toroidal current density J_p is projected onto a representation space, spanned by a suitable basis of n_p elementary currents:

$$J_p(\mathbf{x}) \cong \tilde{J}_p(\mathbf{x}) = \sum_n I_n J_n(\mathbf{x}) \tag{4.2.1}$$

where **x** represents the usual spatial co-ordinates, $J_n(\mathbf{x})$ are the base current densities and I_n are the intensities of the elementary currents, if assuming that the J_n's are characterised by unitary integrals on their support.

A further set of n_e active currents models the external coils; such currents are assumed to be known, while the currents induced in the metallic structures are supposed at this stage to be negligible.

Note that the equivalent currents are able to approximate the magnetic configuration in a neighbourhood of the probe locations; however there is no equivalence in terms of the equilibrium of the forces acting on the plasma because no plasma model is considered here. The equivalent currents representation will be analysed in detail in the following due to its capability to efficiently represent both the magnetic and the non magnetic (like polarimetric) measurements.

5. THE EQUIVALENT CURRENTS METHOD IN THE MAGNETIC CONTOUR IDENTIFICATION

The expansion coefficients I_n in (4.2.1) are computed in order to approximate the actual magnetic measurements, after the contribution of the active currents has been subtracted:

$$\mathbf{G}_p \mathbf{i}_p = \mathbf{b}_m - \mathbf{G}_e \mathbf{i}_e = \mathbf{b} \tag{5.1}$$

where $\mathbf{i}_p$ is the vector of the n_p unknown coefficients I_n, $\mathbf{b}_m=[\mathbf{B},\boldsymbol{\psi}]^T$ is the vector of the m_{MM} magnetic measurements (MM: pick-up coils and flux loops respectively), and $\mathbf{G}_e$, $\mathbf{G}_p$ are the Green matrices linking the effect of the active external currents $\mathbf{i}_e$ and the elementary currents $\mathbf{i}_p$ to the magnetic measurements [12].

Being the magnetic probes located in distinct points, the m_{MM} equations are linearly independent and then $\mathbf{G}_p$ is full-ranked; however $\mathbf{G}_p$ is usually an *ill-conditioned* matrix, and large oscillations both in the solution currents and in the identified plasma contour are expected. To reject to the measurement noise, it is then convenient to over-determine the linear system (5.1) by choosing $m_{MM}>n_p$. A truncated singular value decomposition (TSVD) is then required to afford the problem resolution [13]. From the equivalent plasma current the flux map and finally the plasma boundary are then estimated.

Different choices are possible for the representative base: the most common is constituted by a set of filamentary coils but, as an alternative, a constant piecewise modelling of the plasma current profile can be adopted and, in this case, each element of

the base can be regarded as a flat current distribution defined over a solid toroid with triangular cross-section. Both the solutions present advantages and drawbacks: the filamentary currents represent a somewhat simpler base, leading to faster identifications, while the solid triangular elements allow the magnetic field inside the plasma to be represented with a smoother spatial variation. In any case, both the bases are able to correctly represent the first moments of the actual current distribution, and for this reason are suitable candidates for the reconstruction of the plasma boundary.

Together with the choice of the base currents shape, the effectiveness of the plasma identification process depends strongly on other characteristics of the EC base. As a matter of fact, the higher is the number of terms in the base, the higher should be the accuracy, but the higher is also the expected computational cost. In addition, the quality of the reconstruction depends on the location of the elementary currents. Finally, the reconstruction effectiveness is also influenced by the number of eigenvalues considered in the TSVD.

Note that if some plasma parameter characterising the internal current distribution is required, a full MHD analysis would be necessary if only magnetic measurements are available. On the other hand, it is possible to gain information on the plasma internal magnetic configuration trough a set of different measurements, such as polarimetric ones.

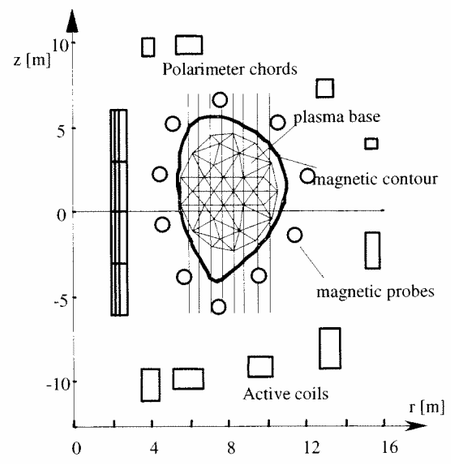

Fig. 5.1 Schematics of a Tokamak in a poloidal cut-plane; the plasma region and the active coils are shown together with the magnetic probes and vertical polarimetric chords.

In Fig. 5.1 a schematic view of the ITER Tokamak cross-section is provided, including both magnetic and polarimetric (PM) measurement systems, the set of active coils and, in addition, a possible set of triangular shaped coils to be used as EC for plasma current representation.

For the m_{PM} polarimetric measurements, a set of m_{MP} linear equations, to be satisfied in a RMS sense, can be written:

$$\mathbf{P}_p \mathbf{i}_p = \mathbf{p}_m - \mathbf{P}_e \mathbf{i}_e = \mathbf{p} \tag{5.2}$$

where $\mathbf{p}_m$ is the vector of PM along a set of vertical chords $\mathbf{l}$ due to the external currents $\mathbf{i}_e$ and to the plasma currents $\mathbf{i}_p$. The matrices $\mathbf{P}_p$ and $\mathbf{P}_e$ describe the contributions to the total polarisation angle rotation due to $\mathbf{i}_e$ and to $\mathbf{i}_p$ respectively. The choice of the chords impacts on the $\mathbf{P}$ matrices, and different chords may be optimal for different plasma configurations [14].

The PM can be included in the plasma reconstruction procedure based on magnetic measurements, by adding to the linear equations (5.1) the further set of linear equations (5.2). The resulting linear system of $m=m_{MM}+m_{MP}$ equations in n_p unknowns becomes:

$$\mathbf{A}\mathbf{i}_p = \mathbf{y} \tag{5.3}$$

where the $m \times n_p$ matrix $\mathbf{A}$ summarises the equations from the magnetic and the polarimetric measurements; the m vector $\mathbf{y}$ represents the corresponding measurements, not including the known effect due to the external coils currents $\mathbf{i}_e$.

The two types of measurements are significantly different and should be used together in such a way to extract from each of them the most useful information. The PM are usually limited in number and are not able to provide themselves a suitable magnetic boundary reconstruction. On the other hand, the MM alone are well suited for magnetic boundary estimate, but are totally unable to give any estimate about the internal plasma current density distribution; therefore the PM could be profitably included to perform such a task.

To treat the polarimetric measurements, the representation of the plasma electromagnetic behaviour has to be approximated by adopting a suitable base of equivalent plasma current. The base chosen here is composed by a set of axisymmetric currents of triangular cross-section located in a region where the plasma is likely to be found. The field inside a triangle is computed as a linear interpolation among the three nodes.

System (5.3), as already anticipated, is ill conditioned, and regularisation procedures must be adopted in order to obtain smooth (and meaningful) solutions. The aim of the regularisation method is to approximate the ill-conditioned matrix $\mathbf{A}$ with a better conditioned matrix. A key role in the computation of the approximating matrix is played by the extent of the measurement errors $\delta\mathbf{y}$, which can be accounted for by the pre-multiplication of the residual vector in (5.3) by the diagonal matrix of the measurements standard deviations $\Sigma=\mathrm{diag}(\sigma_i)$. In this way it is possible to keep into account the different uncertainties affecting the different measurement systems. The system (5.3) then turns into:

(5.4) $$\Sigma \mathbf{A} \mathbf{i}_e = \Sigma \mathbf{y}$$

To obtain a least squares solution of (5.4) within an accuracy commensurable with the uncertainties of the data, the Truncated Singular Values Decomposition technique has been adopted, by keeping into account just the highest k matrix eigenvalues. The integer k is the truncation index, usually selected such as $k< min(m,n_p)$, but a better rule is to choose k in order to neglect the smaller singular values responsible of the ill-conditioning of the matrix $\Sigma \mathbf{G}_e$. However if a small truncation index assures a regular solution, the corresponding residual vector norm in (5.4) increases becoming unacceptable. Therefore a good compromise between the two conflicting conditions must be found.

5.1. Optimal base allocation criteria

The position and the number of the EC heavily impact the performance of the method. To help estimate such effect, a number of numerical analysis have been performed, by varying the characteristics of a representation basis composed of 26 axisymmetric filamentary current loops, uniformly distributed around a circumference centred in C(r_c, z_c) and with radius R. Different locations of the base centre, and different base radii have been considered in order to generate various bases; an example is reported in Fig. 5.1.1(a).

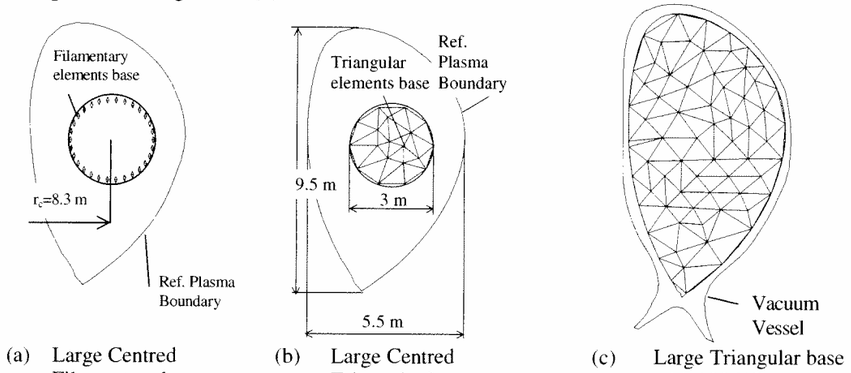

(a) Large Centred Filamentary base (b) Large Centred Triangular base (c) Large Triangular base with 100 EC

Fig. 5.1.1. A sketch of a typical filamentary base (a), of a typical triangular base (b), and large triangular base (C). In (c) also the trace of the vacuum vessel is reported.

The various bases have been used to reconstruct the plasma magnetic contour of a reference X-point equilibrium configuration (in the following "Large Centered", LC), corresponding to the "flat-top" part of the nominal ITER plasma discharge. In the case of filamentary currents, m_{MM}=40 magnetic measurements have been considered while no PM are used. From the solution currents $\mathbf{i}_e$ the approximating magnetic boundary is computed by means of a flux map; the RMS distance δ (metric error) between the points of the approximating magnetic contour and of the reference

magnetic contour is computed for the different bases as a quality index of the identification method. Table I summarises this quality index together with the truncation index k selected.

TABLE I
Assessment of the optimal base allocation alghorithm

26 filaments	(r_c, z_c), R [m]	k	δ [m]
Small cent.	(8.30, 1.35), 0.7	9	0.069
Large cent.	(8.30, 1.35), 1.5	9	0.070
Small up	(7.50, 3.00), 0.7	18	0.572
Large up	(7.50, 3.00), 1.5	18	0.442
Small down	(7.50, 0.30), 0.7	11	0.104
Large down	(7.50, 0.30), 1.5	11	0.086

The accuracy of the measurements is considered here of 0.2 % for the pick-up probes and of 0.1 % for the flux probes, while the full scale range is 2 T and 300 Wb respectively; within this accuracy the minimum number of k corresponds to the base centred with respect to the actual plasma centroid and it guarantees the lowest RMS metric error on the identified magnetic contour.

As an alternative to the filamentary base, we have considered a triangular base, constituted by a set of massive triangular coils, located inside a circle contained in the plasma region (see Fig. 5.1.1(b)). Table II reports results analogous to Table I for a base of 26 triangular cross-section currents with parameters similar to the filamentary base. The performance of such a triangular base is very similar to that of the filamentary one.

TABLE II
Assessment of performance for the triangular base

26 triangles	(r_c, z_c), R [m]	k	ϕ [Wb]	δ [m]
Small cent.	(8.30, 1.35), 0.7	10	0.012	0.068
Large cent.	(8.30, 1.35), 1.5	10	0.012	0.068
Small up	(7.50, 3.00), 0.7	18	0.085	0.726
Large up	(7.50, 3.00), 1.5	18	0.059	0.472
Small down	(7.50, 0.30), 0.7	11	0.015	0.113
Large down	(7.50, 0.30), 1.5	11	0.016	0.072

Table III reports on the other hand a direct comparison among a filamentary base, a triangular base with the same characteristics and a second filamentary base with filaments located at the barycentres of each triangle. The results obtained show a substantially equivalent behaviour among the filamentary basis and the triangular base.

TABLE III
Comparison among filamentary and triangular bases

Base description	(Rc, Zc), r [m]	k	ϕ [Wb]	δ [m]
21 filaments	(8.30, 1.35), 1.5	9	0.011	0.068
21 fil. in the baric.	(8.30, 1.35), 1.5	9	0.013	0.070
21 triangles	(8.30, 1.35), 1.5	9	0.010	0.068

It has been shown in literature [14] that if a combination of MM and PM is used, the best results in the identification of the plasma magnetic boundary are obtained when the equivalent currents fill a good approximation of the actual plasma magnetic boundary (see Fig. 5.1.1(c)); in this case, due to the presence of the PM, the base is made of 100 massive axisymmetric currents with triangular cross-section in order to avoid singularities in the computation of the field or the flux in points very close to the filamentary equivalent currents. The required estimate of the boundary could be provided, for example, by an initial identification from MM only.

The contribution of the PM is particularly effective for the approximation of the internal plasma current density distribution. The capability of the combination of m_{PM}=11 (class 0.3 %, full scale range 13 a.u.) and m_{MM}=20 (same accuracy as reported above) to help in the identification of the plasma current density profile is shown in Fig. 5.1.2: the PM provide a peaked distribution of the equivalent current density (Fig. 5.1.2(b)), in accordance with the actual reference plasma current distribution (Fig. 5.1.2(a)), while with MM only the identified equivalent current density is almost flat (Fig. 5.1.2(c)); however the RMS metric error δ is 0.08 m in both the identifications, with and without the PM.

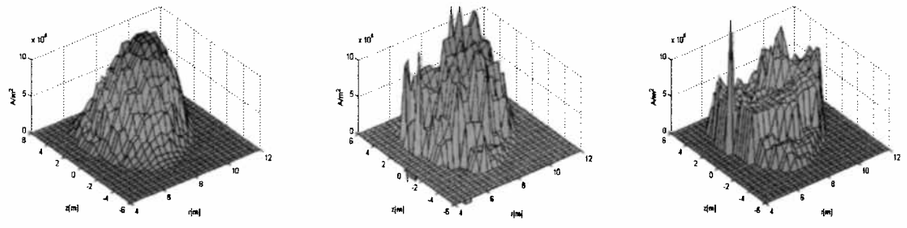

(a) Reference current Density (b) Reconstructed current density (c) Reconstructed current density with MM only.

Fig. 5.1.2. An example of plasma current profile reconstruction, either using (b) or not using (c) the Polarimetric Measurements.

The numerical experiments proved that the PM need a sufficiently large number of equivalent currents, compatibly with the space variation of the actual plasma current density to be identified; in our case a number of n_p=100 equivalent currents was adequate.

Finally, we have assessed the effect of the truncation on the pseudo-inverse calculation by varying the number k of retained eigenvalues for different radii of the circumference where the filaments are located: R=0.7 m and R=1.2 m have been considered. The results of such a study are reported in Fig. 5.1.3; two sets of curves are displayed: the first set is relative to a circular base centred in the centroid of the reference plasma, while the second is relative to an upward displaced base. Note that we have also considered bases with radii lower than 0.7 m, but below this limit the reconstruction becomes rapidly very poor due to the cancellation effect of intense currents of opposite sign close each other.

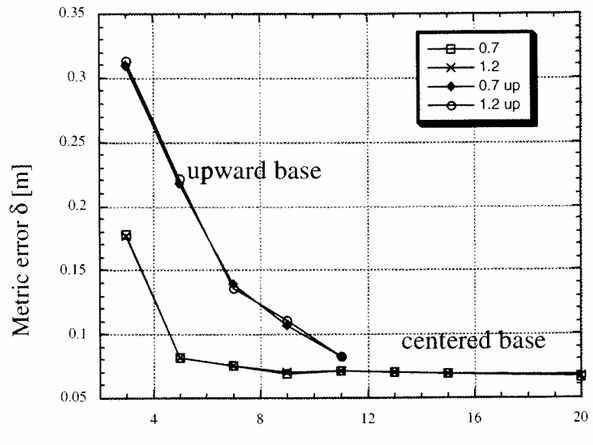

Fig. 5.1.3. Metric error against the number of retained eigenvalues for different number of equivalent currents (filaments).

From the presented results we can summarise that the number k of retained eigenvalues, chosen accordingly to the idea of selecting the eigenvalues on the base of the measurement error, is adequate to correctly represent the plasma boundary within the specified accuracy. On the other hand, the number of base currents should be larger than the number k of eigenvalues required to cope with the specified accuracy, to extract just the first k valid ones.

Note that no improvement of the reconstruction quality is obtained when adding further currents above a certain threshold. In addition, the base currents should fill a region as large as possible, and should be placed as close as possible to the actual plasma centroid (if known), or in the geometric centre of the plasma chamber if no other information is available. Finally, no particular advantage is taken if adopting triangular currents, and the filaments should then be preferred thanks to their simplicity, if only geometrical parameters are required.

5.2. ADAPTIVE BASE ALLOCATION

The criteria exposed above can be considered as suggestions to profitably place the EC when the plasma boundary is, at least in a rough way, known. An alternative approach is to solve the identification problem starting from a tentative base of arbitrary allocation and adaptively modify it until the discrepancy between two successive identified magnetic contours is within a prescribed tolerance ε [15]. As measurements, only MM or a combination between MM and PM can be used.

The adaptive basis placement algorithm can be summarised in the following steps:

step 0: select an initial base B_0; in order to allow the use of PM, a base with triangular cross-section currents has to be adopted; consequently a magnetic contour C_0 is identified.

step h: the area enclosed by the previous contour C_{h-1} is meshed with triangular elements, providing a new base B_h from which a new magnetic contour C_h can be identified.

stop condition: when the difference of the RMS metric error δ_h between C_{h-1} and C_h is not larger than ε; in order not to tackle the algorithm, the absolute discrepancy δ with respect to the reference contour has been considered instead (10 cm is assumed here) together with a maximum number of iterations (10).

When the initial base is badly allocated, the system matrix becomes very ill-conditioned; therefore an upper limit (below 10^9) to the condition number has been imposed causing a consequent upper limit of the truncation index k.

In the following, an example of such an adaptive procedure is reported, in the case of m_{MM}=40 and m_{PM}=11, with the usual accuracy and full scale range. When the LC ITER equilibrium is considered as reference case, the algorithm proved to be convergent within 2-3 iterations to a good approximation of the actual magnetic contour independently from the allocation of the initial base B_0, both with the MM only and with the combination of MM and PM.

The role played by the PM, when combined with the MM, in the convergence of the adaptive algorithm can be appreciated if the plasma to be identified is far from the initial estimate. In order to help appreciate the effect of the PM, a Small Displaced (SD) equilibrium with limiter configuration, corresponding to the termination phase of the ITER discharge, has been considered as reference instead of the LC equilibrium.

In this case the identification procedure is not able to provide an acceptable plasma boundary (RMS metric error δ>10 cm) within 10 iterations by means of magnetic measurements only; whilst using MM integrated with PM, the adaptive procedure is able to converge to a good magnetic boundary estimate (RMS metric error δ<2 cm) within 5 iterations, starting from the same initial bases. Such a bad starting base has been chosen in order to appreciate the robustness of the adaptive procedure.

In Fig. 5.2.1(b) the sequence of each of the 5 iteration steps for a typical case is shown using MM and PM, while in Fig. 5.2.1(a) the same iteration steps are shown in the case of MM only: without the PM the adaptive identification fails to converge, and starts to oscillate after 5 steps.

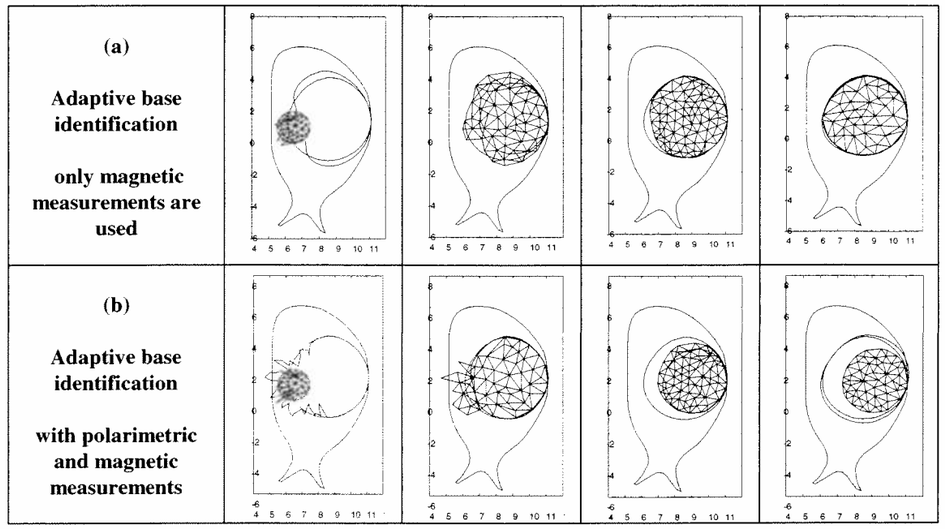

Fig.5.2.1. The sequence of snapshots (from left to right) represents at each iteration step the adapted base, the identified and reference magnetic boundary; using MM and PM the adaptive identification method is convergent (row a), while using only MM (row b) the adaptive identification method does not converge.

Of course, the adoption of an adaptive strategy slows down the identification procedure, and then must such a sophisticated approach must be adopted only when the identification unit must follows severe plasma shape variations.

6. PROBES OPTIMIZATION

A further issue that has been addressed in the due course of the project is a critical analysis of the probe positioning around the plasma chamber, in order to optimise their allocation with respect to the identification unit needs. The purpose of this section is then to sketch the results obtained using a possible strategy, proposed in literature, to optimise the performance of the magnetic probes [16]. The optimality criterion is defined in terms of reliability of the flux map reconstruction, noise rejection capability, and robustness against possible damages. In addition, the number of probes in the set must be kept minimal.

Only the flux probes have been examined in this study for the sake of simplicity, having the magnetic field map very similar smoothness properties.

The proposed strategy is organised as follows:

a. Identify a *suitable region* for the probes allocation;
b. Create a *data base of flux maps*;
c. Identify the *minimum number of probes*;
d. *Optimise the probe positions* in such a way to attain the maximum amount of information while counteracting the effect of the measurement noise and of probes malfunctioning.

With reference to the ITER project, the suitable region (point a) has been chosen as the line γ interpolating the actual ITER probe locations, in order to keep the mechanical constraints satisfied.

A number of flux maps (1000) has then been generated (point b), by representing the plasma current with a suitable EC expansion, and by imposing just a rough equilibrium condition (no vertical force on a filament located in the plasma centroid and carrying the whole plasma current), in order to speed-up the computations, the main interested being in this study just in the topological aspect of the flux maps.

The number of probes (point c) has been chosen, on the basis of the Shannon theorem, as twice the number of terms required in the Fourier expansion of the magnetic flux over γ to obtain an error between the actual flux map and its Fourier expansion below the measurement uncertainty.

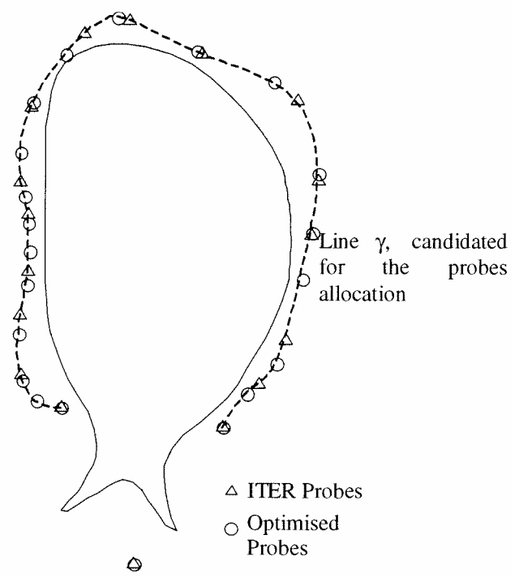

Fig.6.1. Results of the probes allocation strategy: the "suitable region" γ, and the optimised probes ('o'), compared with the ITER probes ("Δ"), are reported.

Finally, the optimal probe locations (point d) have been selected from a pool of possible measurement points uniformly distributed along γ as those minimising the mutual dependence of the measurements. The mutual dependence between two different points has been estimated using the covariance of the flux values in the points, evaluated on the set of pseudo-equilibria in the generated data base.

As an example, in Fig. 6.1 the optimised locations for 20 probes are reported; in the same figure, also the ITER probes are reported for comparison.

The application of the procedure to the actual ITER design proved that the probes foreseen in the present project represent a good choice, but some margins of improvement are still present.

7. PLASMA CONTOUR IDENTIFICATION IN PRESENCE OF EDDY CURRENTS

The magnetic field measured outside the vessel of the toroidal experimental devices for plasma magnetic confinement is affected by the current distribution induced in the conducting vessel due to the variation of the external coils and plasma currents.

For many of the existing Tokamaks the induced currents can be neglected, being the variations slower of the shortest time constant. Nevertheless this assumption reveals critical in the case of ITER, and suitable techniques must be developed to deal with the currents induced in the passive axisymmetric conducting structures, like the vacuum vessel [17, 18].

A possible approach could be to discretise these conducting structures as a set of axisymmetric massive conductors: the amplitudes of the corresponding currents must be included among the unknowns to be determined through the best fitting procedure.

The inclusion of these further unknowns of course worsen the conditioning of the problem, and any additional information resulting from *a priori* knowledge about the system must be used to help regularising the problem. As an example, it is possible to exploit the knowledge about the time evolution of the current density inside the conductive vessel provided by the magneto-quasi static set of Maxwell equations. To this purpose, the passive structures can be schematised by a LR equivalent lumped parameters network, which prescribes the time evolution of the vessel currents, and the related equations included in the problem statement.

Of course, the nature of the information provided by the measurements and by the eddy currents effect in the passive structures is different, and consequently different mathematical models must be adopted for their description.

The first model consists on a set of linear algebraic equations, used to represent the magnetic measurements. According to this model the following equation can be written:

$$\mathbf{G}_p\mathbf{i}_p + \mathbf{G}_v\mathbf{i}_v = \mathbf{b}_m - \mathbf{G}_e\mathbf{i}_e = \mathbf{b} \tag{7.1}$$

being **b** the known vector of the magnetic measurements, and $\mathbf{i}_e$ the known vector of the currents in the active external coils as a functions of time; $\mathbf{i}_v$ and $\mathbf{i}_p$ are the arrays of the unknown currents in the passive conductors (vessel) and the equivalent plasma currents respectively. The $\mathbf{G}_p$, $\mathbf{G}_v$, $\mathbf{G}_e$ matrices link the array of the measurements **b** with $\mathbf{i}_p$, $\mathbf{i}_v$ and $\mathbf{i}_e$ current amplitude arrays respectively: in general these are not square matrices, depending on the number of the measurements and on the number of the equivalent plasma currents, passive currents and active currents adopted in the model of the device.

The second model consists on a set of linear differential equations describing the LR dynamic model of the passive structures:

$$\mathbf{M}_p \frac{d\mathbf{i}_p}{dt} + \mathbf{M}_v \frac{d\mathbf{i}_v}{dt} + \mathbf{M}_e \frac{d\mathbf{i}_e}{dt} + \mathbf{R}\mathbf{i}_p = 0 \qquad (7.2)$$

being $\mathbf{M}_p$ and $\mathbf{M}_e$ the matrices of the mutual inductances between the passive conductors and the equivalent plasma and active currents respectively; **M** and **R** represent the mutual inductance and resistance matrices of the passive conductors.

The crucial issue is the integration of the linear algebraic equations (7.1) with the differential equations (7.2) in order to determine numerically the unknown quantities $\mathbf{i}_p$ and $\mathbf{i}_v$. The flux map generated by the identified currents is then evaluated and the plasma magnetic boundary can be determined.

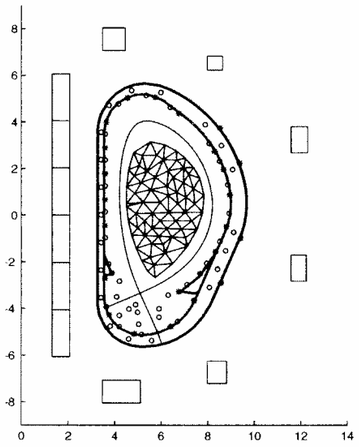

Fig. 7.1. ITER FEAT radial cross-section: 12 active conductors, vacuum vessel, probe locations, plasma equivalent currents (triangular cross-section) and plasma magnetic separatrix.

To test the method, a set of plasma numerical equilibria have been considered as reference, simulated by means of the MAXFEA finite element code [19] in the case of the ITER FEAT geometry. In Fig. 7.1 the model representing the 12 active conductors and the discretisation of the vacuum vessel (120 massive conductors for the inner/outer vessel, 9 for the inner/outer wings) is shown together with the probe

locations ("o" pick-up coils, "*" flux loops), plasma equivalent currents (triangular cross-section) and plasma magnetic separatrix.

In fig. 7.2 the reconstructed eddy currents inside some of the conducting structure elements (6 inner and 6 outer vacuum vessel elements) are reported together with the evolution of the currents in the same elements evaluated by means of the MAXFEA finite element code.

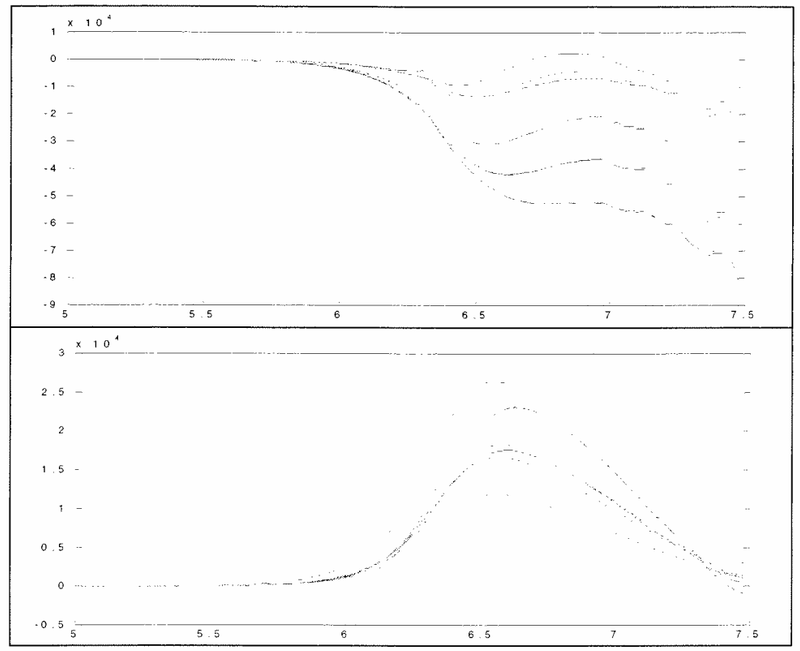

Fig. 7.2. Time evolution of the eddy currents of 6 inner (up) and 6 outer (down) vacuum vessel elements: reconstructed and evaluated by means of the MAXFEA finite element code.

8. CHARGED PARTICLES TRAJECTORIES

A fascinating alternative to conventional magnetic field measurements has recently been proposed for the identification of magnetic field profiles in high current plasma discharges [20, 21, 22, 23]. It is based on the analysis of the trajectories of charged projectiles injected across the plasma region. The original application for which the technique was developed is the diagnostic of the focusing field in a plasma lens, used as final stage in an ion beam accelerator chain. It is then easy to imagine that small bunches of accelerated charged particles can act as the «projectiles» needed by the

technique. Anyway, the application of the technique to the identification of magnetic fields in Tokamaks is currently under investigation.

The measurement principle is based on the detection of deflections in the particles trajectories trough one or more scintillators (devices able to detect charges passing through their sensing surface), placed at the exit of the plasma region. From the comparison of input and output position and momentum, it is possible to identify the force field producing such trajectories.

As most of the indirect field measurement principles, the reconstruction method is based on the resolution of an inverse problem, namely the inversion of the particles motion problem: the magnetic force (and then the magnetic field, as the other motion parameters are known) acting on the particle is the unknown to find out from the knowledge of the input-output positions data couples.

Of course, a suitable representation of the field map is required to regularise the problem and to obtain a discrete formulation, to be implemented and solved via numerical procedures. In 2-D symmetric cases a good choice for the unknown could be the magnetic vector potential **A**, characterized by one component only, and expressed by means of its polynomial expansion in terms of the in-plane co-ordinates.

The identification procedure is based on the minimization of the RMS error between the trial and the measured output trajectories data.

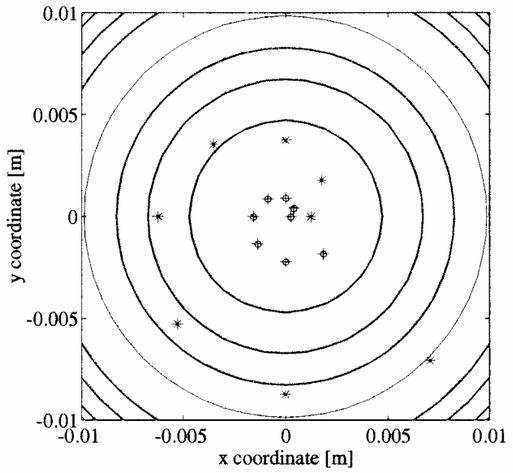

Fig. 8.1. Example of the field map reconstruction: the vector potential of a magnetic field map with circular force lines is reconstructed using a second order polynomial $p(x,y)$, starting from the deflections of 16 charged particles. Reference and identified field lines are not distinguishable within the adopted resolution. Input particle positions ("*"), reference output positions ("+") and reconstructed output positions ("o") are also reported.

Fig. 8.1, as an example of the possibilities offered by the exposed method, presents the results of the identification for a 2-D test case, in which the coefficients of the expansion fitting a field with circular force lines are determined. For the identification, 16 particles are used, with input positions along a spiral.

In the course of the project, the possibility of the method have been explored, with reference either to 1D and 2D geometry. It is presently under development the extension to the toroidal axisymmetric geometry characterising the ITER Tokamak.

9. CONCLUSIONS

The problem of the plasma magnetic contour identification has been analysed, showing the benefits of the integration between magnetic and non magnetic measurements. Among the non magnetic measurements the polarimeters have been considered, which provide information on the internal plasma configuration.

To obtain a smooth approximation of the magnetic contour, specific regularisation methods have to be adopted, based on proper plasma model or alternatively on a least squares approach.

In the case of the eddy currents in the passive conducting structures, an electromagnetic lumped parameters model can be profitably used as regularisation method.

The problem of optimal probe placing have also been faced and solved.

An alternative to conventional magnetic configuration identification has been proposed, based on the analysis of the trajectories of charged particles.

10. REFERENCES

[1] J.A. Wesson: "Tokamaks", Oxford Clarendon Press, 1987.

[2] A. Stella et al.: "An Integrated Approach to Control of Magnetically Confined Plasmas", *Proceedings of 21st Symposium on Fusion Technology* (SOFT 2000), Madrid (Spagna), 11-14 September 2000.

[3] De Kock L.C.J.M., Kuznetsov Yu.K., (1996): "Conference and Symposia: Magnetic Diagnostics for Fusion Plasmas", *Nuclear Fusion*, Vol.36, N° 3, pp. 387-400.

[4] De Marco F., Segre S. E., (1972), *Plasma Phys.*, vol. 14, pp. 245.

[5] B.J. Braams: "The Interpretation of Tokamak Magnetic Diagnostics", *Plasma Physics and Controlled Fusion*, Vol. 33, N. 7, pp. 715-748, 1991.

[6] M. Bagatin G. Chitarin, D. Desideri, A. Murari, R. Piovan, L. Zabeo: "Integration of magnetic and non-magnetic measurements for current profile reconstruction in RFX", *Review of Scientific Instruments*, Vol. 72 (2001) pag. 426-429.

[7] R.Piovan: "Ricostruzione dei profili di campo magnetico e densità di corrente nel plasma", *Internal Report SE61 of Istituto Gas Ionizzati*, Padova, 1997 (in italian).

[8] D. Desideri, L. Zabeo, M. Bagatin, G. Chitarin, R. Piovan: "A fast code using non-magnetic measurements for RFX current and magnetic field profile reconstruction2, submitted to the 13th Compumag Conference, Evian (2001).

[9] Swain D.W., Neilson G.H., (1982): "An Efficient Technique for Magnetic Analysis of Non-Circular, High-Beta Tokamak Equilibria", *Nuclear Fusion*, vol. 22, n° 8, pp. 1015-1030.

[10] M. Bagatin, A. Formisano, R. Martone, A. Stella, F. Trevisan: "Improvements to the Plasma Identification in Fusion Devices via Inclusion of non Magnetic Diagnostics", *Proceedings of ICEAA '99*, Turin, 13-17 September 1999.

[11] P. Bettini, A. Formisano, R. Martone, A. Stella, F. Trevisan: "Combined Reconstruction Techniques for Geometrical and Magnetical Characteristics of Thermonuclear Plasmas", *Proceedings of International Workshop on "Optimisation and Inverse Problems in Electromagnetism" (OIPE 2000)*, Turin, 25-27 September 2000; to be published on Compel.

[12] P. Bettini, F. Bellina, A. Formisano, R. Martone, A. Stella, F. Trevisan: "Model Parameter Impact on Plasma Identification by means of Equivalent Currents from External Magnetic Measurements", *Proceedings of Numelec 2000*, 20-22 marzo 2000, Potiers (Francia); to be published on *European Physics Journal*.

[13] R.J. Hanson: "A Numerical Method for Solving Fredholm Integral Equations of the First Kind Using Singular Values", *SIAM Journal of Numerical Analysis*, Vol. 8, N. 3, pp616-622, 1971.

[14] P. Bettini, A. Formisano, R. Martone, F. Trevisan, A. Stella: "Impact of Positioning and Number of Polarimetric Measurements on the Plasma Reconstruction in Fusion Devices", *Proceedings of EMF 2000*, Gent (Belgium), 17-19 May 2000, to be published on Compel.

[15] P. Bettini, A. Formisano, F. Trevisan: "An Adaptive Method to Identify the Plasma Magnetic Contour from Magnetic and Polarimetric Measurements", *Proceedings of 21st Symposium on Fusion Technology* (SOFT 2000), Madrid (Spain), 11-14 September 2000.

[16] A. Formisano, R. Martone, F. Trevisan: "Optimal Placement of Probes in Magnetostatic Reconstruction, the Case of Plasma Identification in Tokamaks", *Proceedings of 9th International IGTE Symposium on Numerical Field Calculation in Electrical Engineering*, Graz (Austria), 11-13 September 2000, to be published on Compel.

[17] A. Formisano, R. Martino, R. Martone, R. Fresa: "Improvement of Plasma Identification in Tokamak Devices with Dynamical Information", *IEEE Trans. on Magnetics*, Vol. 10 N° 3, July 2000.

[18] A. Stella, F. Trevisan: "A Method for the Identification of the Plasma Magnetic Boundary in Machines for Fusion Research", *IEEE Trans. on Magnetics*, Vol.36, n.4, July 2000, 780-784.

[19] Barabaschi P.: "The Maxfea code", Plasma Control Technical meeting, Naka, Japan, April 1993.

[20] L. Corti, M. de Magistris, A. Formisano, M. Stetter: "An Inverse Formulation for the Identification of Magnetic Field Profiles in Plasma Lenses", *IEEE Trans. on Magnetics*, Vol. 34 N° 5, September 1998, pp. 2897-2900.

[21] M. de Magistris, A. Formisano: "Identification of 1-D Magnetic Field Profiles in High Current Plasmas", *Compel*, Vol. 18, N° 3, pp. 275-284, 1999.

[22] M. de Magistris, A. Formisano: "Identification of 2-D Magnetic Fields via Analysis of Charged Projectile Trajectories", *Proceedings of Compumag '99*, Sapporo (Japan), 25-28 October 1999.

[23] M. de Magistris, A. Formisano: "Identification of Magnetic Fields by Charged Projectiles Data", *Proceedings of International Workshop on "Optimisation and Inverse Problems in Electromagnetism" (OIPE 2000)*, Turin, 25-27 September 2000.